Comput. Math. Applic. Vol. 13, No. 1–3, pp. 97–110, 1987
Printed in Great Britain

0097-4943/87 $3.00 + 0.00
Pergamon Journals Ltd

AN APPROACH TO THREE-DIMENSIONAL AIRCRAFT PURSUIT–EVASION

M. D. ARDEMA
Santa Clara University, Santa Clara, CA 95053, U.S.A.

N. RAJAN
Sterling Software, Palo Alto, Ca 94043, U.S.A.

Abstract—An algorithm for obtaining a state-feedback control law for near-optimal aircraft pursuit evasion in three dimensions is outlined. Key features of the approach are the use of singular-perturbation ideas to decouple the dynamics of each of the two players and the use of a reference frame that decouples the slow subsystem extremals of one player from those of the other. The resulting subproblems are then tractable for closed-loop solution, and the solutions may be combined to give a control law feasible for real-time implementation. Compared with past analyses of pursuit–evasion games, our dynamic model is higher order and more realistic; therefore, our results should be of practical value for aircraft control. And because we use fewer time-scales than were used in past analyses of flight dynamic problems by singular-perturbation methods, our algorithm should be more accurate.

1. INTRODUCTION

Most investigations in which the theory of differential games was used to model air-to-air combat were based on deterministic, perfect-information pursuit–evasion games. In the pursuit–evasion formulation, (i) there are two combatants, or players, (ii) the roles of the players are fixed and predetermined, one being designated the pursuer and the other the evader, and (iii) the pursuer's objective is to minimize the time-to-capture (assuming capture is possible) and the evader's is to maximize it; thus the game is two-person and zero-sum.

One of the first pursuit–evasion problems to receive attention was the game of two cars, in which the two players move in the same plane with fixed speeds and bounded turn rates [1–5]. Independently, the differential-turning game was developed; in this formulation the energies of the two players and their relative heading are treated as state variables [6–9]. As models of air combat, these two approaches are quite different, the first focusing on positional advantage and neglecting vehicle dynamics and the second focusing on the interplay between energy management and turning while ignoring position [10]. Although the results of these analyses are of qualitative interest, both approaches use third-order dynamic models and consequently are of limited value in determining optimal tactics in actual air combat.

More recently, a pursuit–evasion game with variable-speed point-mass aircraft models in a horizontal plane (a fifth-order model in relative coordinates) was investigated [11–15]. The approach hinges on the use of a coordinate system that in a certain sense uncouples the extremal paths of the pursuer from those of the evader. This allows open-loop extremal trajectory maps for each player to be generated independently; these maps then can be combined in a common coordinate system to obtain isochrones and feedback controls. A special case of these results is the target–interception problem of optimal control, in which the evader's motion is fixed and known to the pursuer; in this case we call the pursuer the interceptor and the evader the target.

Because the target–interception problem is computationally easier than pursuit–evasion (requiring the generation of one extremal trajectory map instead of two), many results have been illustrated in terms of target interception. For example, Fig. 1 [14, 15] shows a feedback control solution for the case of an initial target speed of Mach number (M) 1.0, an initial interceptor speed of M = 0.9, and an initial relative heading of 135°. Shown in the figure are the optimal bank controls of the interceptor as a function of the position of the target relative to the interceptor, as well as the isochrones (loci of constant time-to-capture). Capture is defined to occur when the interceptor gets within 316 m of the target. A piece of an isochrone for a pursuit–evasion problem is shown in relative coordinates in Fig. 2. It would take the computation of many such isochrones to construct a feedback chart such as the one shown in Fig. 1.

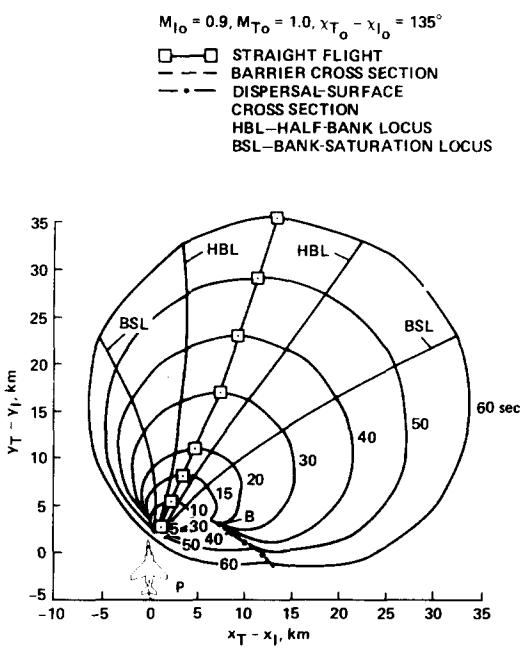

Fig. 1. Feedback bank control chart for optimal target interception in a horizontal plane (F4-C aircraft).

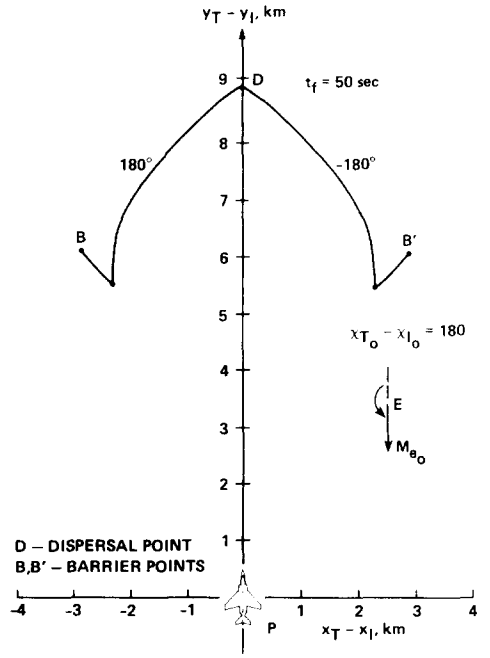

Fig. 2. A portion of an isochrone for optimal pursuit evasion in a horizontal plane (F4-C).

The major shortcoming of the analysis just described is its restriction to a horizontal plane. Since it is well known that vertical-plane maneuvering is important for high-performance aircraft, this restriction is a severe one. The purpose of this paper is to outline an approach to obtaining near-optimal feedback controls in deterministic, perfect-information, three-dimensional aircraft pursuit–evasion (3DAPE).

If both the pursuer and evader are modeled as constant-weight point-masses, the state equation of the three-dimensional game is twelfth order (sixth order for each player). Consequently, the open-loop extremals satisfy a 24th order, two-point boundary-value problem in 12 state and 12 adjoint variables. Although this is a computational problem of great complexity [10], numerical solutions of similar problems have been obtained [16, 17]. In order to achieve a solution to the 3DAPE problem in a feedback form suitable for real-time implementation, however, simplifications are required.

Our approach to making 3DAPE feedback solutions tractable is based on the singular-perturbation technique of time-scale separation of the dynamics of each aircraft [18–20] and on the use of the decoupling coordinate system introduced in [11–15]. In the interests of accuracy, our guiding principle is to use as few time-scales as possible. The equations of motion are written in a singularly perturbed form such that the reduced (outer, slow) problem is the three-dimensional energy-state (3DES) dynamic model [18, 21]. The same coordinate system that decouples the players' extremals in the horizontal plane also decouples the players' extremals in the 3DES case; therefore, solution of the reduced problem is much the same as the solution given in [11–15]. The 3DES formulation contains both the two-cars and differential-turning formulations as special cases.

Under the key assumption that the capture (termination) condition is independent of the boundary-layer (inner, fast) variables, the boundary-layers of each aircraft are independent of the other. In our analysis, we treat the boundary-layer equations in two ways, depending on the proximity of the current state to the 3DES solution. For the initial boundary layer and in the regions of large transitions between branches of the 3DES solution, we use complete time-scale decoupling of the variables of the nonlinear boundary-layer system. As is well known, this leads directly to a nonlinear feedback control law [22–25]. In the vicinity of the 3DES solution, we leave the equations coupled, but transform them to a new variable which gives a more accurate estimate of the fast variables on the 3DES solution [26, 27], and finally linearize about the 3DES solution to obtain linear feedback control corrections.

When specialized to the target-interception problem, our approach is similar to two other recent derivations of feedback guidance laws for three-dimensional problems by singular-perturbation techniques [24, 25]. However, both of those other investigations used complete time-scale separation of all variables, differing only in the ordering of the speeds of the variables. In light of recent time-scale analysis [28], such sweeping time-scale separation seems suspect and it is not known how near optimal the resulting guidance laws are. In any case, because of the less severe time-scale decoupling, our algorithm should be more accurate. It is significant, however, that the guidance algorithm in [24] has been extensively simulated [29] and even flight tested to some extent, thus demonstrating that this class of algorithm can be implemented in real time.

Before beginning the detailed development of our algorithm, we wish to point out that pursuit–evasion is a special case of air-to-air combat, in which one of the aircraft has negligible offensive capability. In the more general case, both aircraft have offensive capability and objectives, and that problem is much more complex [30–33]; indeed, there has been no attempt to solve it in three dimensions.

2. DYNAMIC MODELING

We begin with the assumption that each aircraft, the pursuer and the evader, is adequately modeled as a constant-weight point-mass. In the wind system of axes, the motion of each aircraft, or player, is then governed by the equations of motion:

$$\begin{aligned}
\dot{x} &= V\cos\gamma\cos\chi \\
\dot{y} &= V\cos\gamma\sin\chi \\
\dot{h} &= V\sin\gamma \\
\dot{V} &= g(T - D - \sin\gamma) \\
\dot{\chi} &= gn\sin\theta/V\cos\gamma \\
\dot{\gamma} &= g(n\cos\theta - \cos\gamma)/V,
\end{aligned} \tag{1}$$

where $(\dot{}) = \mathrm{d}(\ )/\mathrm{d}t$ and the state variables are horizontal position (x, y), altitude (h), speed (V), heading angle (χ), and flightpath angle (γ) [34]. The thrust and drag per unit weight are given by

$$\begin{aligned}
T &= \beta T_{\mathrm{M}}(h, V) \\
D &= D_0(h, V) + D_i(h, V)n^2.
\end{aligned} \tag{2}$$

The constraints on the control variables β (throttle setting), θ (bank angle), and n (load factor) are

$$\begin{aligned}
0 &\leqslant \beta \leqslant 1 \\
-\pi &\leqslant \theta \leqslant \pi \\
n_{\mathrm{m}} &\leqslant n \leqslant n_{\mathrm{M}} = \min[n_{\mathrm{s}}, \hat{L}(h, V)],
\end{aligned} \tag{3}$$

where n_{s} is the maximum (structural) load factor and $\hat{L}$ is the lift per unit weight as limited by maximum angle of attack, α_{M},

$$\hat{L}(h, V) = C_{L_\alpha}(h, V)\alpha_{\mathrm{M}}\rho(h)V^2S/2W. \tag{4}$$

In this equation, C_{L_α} is the lift-curve slope, ρ is the atmospheric density, S is the wing-reference area, and W is the weight.

Time-scale analysis of (1) reveals that for a typical high-performance aircraft, x and y are the slowest state variables, γ and χ are the fastest, and h and V are of intermediate speed [28]. Our basic approach is to use as few time-scale separations as possible while still leaving each subproblem tractable for real-time implementation. To this end, we introduce the energy variable, defined by

$$E = V^2/2g + h, \tag{5}$$

and replace V by E in the equations of motion. Since E is slow relative to h, we can then put x,

y, χ, and E on the same time-scale (χ is put on this time-scale because of our goal to use as few time-scales as possible). The two faster variables, h and γ, are then put on separate, faster time-scales. The resulting singularly perturbed system is

$$\begin{aligned}
\dot{x} &= V\cos\gamma\cos\chi \\
\dot{y} &= V\cos\gamma\sin\chi \\
\dot{E} &= V(T-D) = P(E,h,n,\beta) \\
\dot{\chi} &= gn\sin\theta/V\cos\gamma \\
\epsilon\dot{h} &= V\sin\gamma \\
\epsilon^2\dot{\gamma} &= gn\cos\theta/V - g\cos\gamma/V,
\end{aligned} \tag{6}$$

where, from (5),

$$V(E,h) = [2g(E-h)]^{1/2}. \tag{7}$$

To zero-order in ϵ, the optimal controls for a system such as (6) can be written as an algebraic feedback law depending on the current state variables and on the adjoint variables of the reduced solution [22–25]. The reduced problem, obtained by setting $\epsilon = 0$, is the energy-state approximation [18, 21]. It is assumed that Theorem 2.2 of [20] holds for (6).

In our approach, the nonlinear guidance law just discussed will be used only when the current state is "far away" from the reduced solution in terms of altitude. When the current state is "near" the reduced solution, we will use a linear guidance law based on boundary-layer analysis of a state system of the equations of motion slightly different than (6). The reduced solution of (6) defines an optimal energy-state path in the (V,h) plane; let this path be denoted by

$$f(h,V) = 0. \tag{8}$$

We then make the change of variable $h \to f$, replace $\sin\gamma$ by γ and $\cos\gamma$ by 1, and put f and γ together on a fast time-scale to get (from [27])

$$\begin{aligned}
\dot{x} &= V'\cos\chi \\
\dot{y} &= V'\sin\chi \\
\dot{E} &= P' \\
\dot{\chi} &= gn\sin\theta/V' \\
\epsilon\dot{f} &= \phi\gamma + \psi P' \\
\epsilon\dot{\gamma} &= g(n\cos\theta - 1)/V',
\end{aligned} \tag{9}$$

where

$$\begin{aligned}
\phi &= Vf_h - gf_V \\
\psi &= gf_V/V,
\end{aligned} \tag{10}$$

and where $h'(E,f)$ and $V'(E,f)$ are to be determined from (5) and (8) and $P'(E,f,n,\beta) = P(E,h,n,\beta)$, $f_h(E,f) = \partial f(h,V)/\partial h$, and $f_V(E,f) = \partial f(h,V)/\partial V$. The reduced problem associated with (9) is the same as that associated with (6), i.e. it is the 3DES, except for the *a posteriori* calculation of γ. For (6), the reduced value of γ is always zero, whereas for (9) it is equal to the actual value along the reduced path. Thus, boundary-layer corrections based on (9) should be more accurate than those based on (6), both because of the less severe time-scaling of (9) and because of the more accurate reduced value of γ. The assumption that γ is small is necessary in order to get a formulation with the 3DES as a reduced problem; this assumption should be quite good since γ has been found to be $<3^\circ$ along the reduced solution in typical cases [27].

Now denote the pursuer and evader by subscripts p and e, respectively, and let $\mathbf{s}_i = (x_i, y_i, E_i, \chi_i)^T$, $i = \mathrm{p}, \mathrm{e}$, and

$$\mathbf{s} = \begin{bmatrix} \mathbf{s}_\mathrm{p} \\ \mathbf{s}_\mathrm{e} \end{bmatrix}.$$

In pursuit–evasion, the cost functional is time-to-capture,

$$J = \int_0^{t_f} \mathrm{d}t, \tag{11}$$

which p desires to minimize and e to maximize, assuming capture to occur. The evolution of the state of each player is governed by a system of equations (6) or (9). The termination time t_f is determined by a capture condition; i.e. a state constraint is imposed such that

$$\mathbf{s}(t) \notin \mathscr{T} \subset \mathbb{R}^8 \quad \forall\, t \in [0, t_f), \tag{12}$$

and

$$\mathbf{s}(t_f) \in \mathscr{T}. \tag{13}$$

Here, $\mathscr{T}$ is the target or capture set. It is essential to our approach that $\mathscr{T}$ be a subset of the slow subspace only, and, therefore, that the coupling between the two players is restricted to the reduced (3DES) problem. The 3DES solution will then contain all the game features of the problem (such as the assumed roles of the players, capturability, and location of barriers and other singular surfaces). The boundary layers of each player may then be analyzed independently; their role is to provide near-optimal transitions to the 3DES solution at the initial time, and between branches of the 3DES solution at later times.

In the following sections, we will consider, in turn, the 3DES problem and the boundary-layer problems associated with (6) and (9).

3. THREE-DIMENSIONAL ENERGY STATE

Setting $\epsilon = 0$ in (6) and (9) leads to the same reduced problem, the 3DES system:

$$\begin{aligned} \dot{E} &= P(E, h, n, \beta) \\ \dot{\chi} &= gn \sin\theta / V \\ \dot{x} &= V \cos\chi \\ \dot{y} &= V \sin X \\ n \cos\theta &= 1. \end{aligned} \tag{14}$$

It is easy to verify that all conditions of Theorem 2.3 of [20] are met and, therefore, that the extremals of (14) will indeed be the same as those obtained by applying necessary conditions to (6) or (9) and then setting $\epsilon = 0$.

Equations (1), (6), (9), and (14) are valid in any inertial reference frame with rectangular Cartesian coordinates (x, y, h). We now adopt an inertial frame such that the pursuing aircraft is at the origin at capture (i.e. at time t_f) and the evader is on the x-axis at a prespecified distance R from the origin (Fig. 3). As shown in [21], this reference frame has the advantage that the terminal and transversality conditions of the pursuer are uncoupled from those of the evader; as a result, we may generate the open-loop extremal solutions of each player independently. The disadvantage is that the frame varies from encounter to encounter, which makes it necessary that the results be transformed into a common, relative reference frame in order that they be useful for constructing feedback controls.

Example 3DES open-loop extremals for an F4-C aircraft were computed in [21] and are shown in Figs 4 and 5. In Fig. 4 are displayed extremal trajectories in the (h, V) plane for several values of E_f and fixed χ_f. Trajectories that start from relatively high values of energy lie entirely on the maximum speed boundary, $V_M(E)$. Trajectories starting from lower values of energy start on the corner speed locus (locus of maximum instantaneous turn rate), $V_c(E)$, then jump to an interior point and quickly transition to V_M. Trajectories that start at low energies start on V_c and end on the terrain limit.

Figure 5 shows the projection of extremal trajectories in the horizontal plane for various values of final heading χ_f, with final energy E_f fixed. All trajectories start (in forward time) with throttle off ($\beta = 0$), corner speed ($V = V_c$), and bank angle saturated. After a few seconds, the throttle is

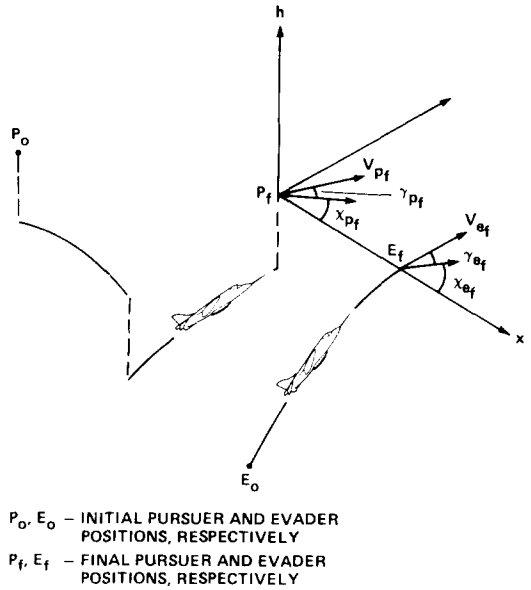

Fig. 3. Encounter-dependent, decoupling, inertial reference frame.

switched to full ($\beta = 1$), and after a few seconds more the speed jumps to maximum ($V = V_M$). Then, the bank becomes unsaturated, and gradually decreases to near zero at termination.

Our approach to constructing feedback solutions to the 3DES problem is (i) to flood the state space with numerical, open-loop solutions for the pursuer in the encounter-dependent, inertial reference frame, (ii) to do the same for the evading aircraft, and (iii) to transform the two solutions into a reference frame fixed to one of the players and plot isochrones in this reference frame to get feedback (state-dependent) control laws. For each player, these control laws are in the form of tabular data giving the controls β, θ, and n in terms of the current relative position $(x_p - x_e, y_p - y_e, \chi_p - \chi_e)$ and the energies of the two aircraft (E_p, E_e). It is during this last step that capture requirements on the relative values of E may be imposed. For example, requiring that $E_p \geq E_e$, or, more appropriately, that $V_m(E_p) \geq V_m(E_e)$, where $V_m(E)$ is the loft ceiling locus, eliminates otherwise optimal pairs of trajectories and consequently reduces the capturability region.

The control laws resulting from the 3DES solution may be written symbolically as $\beta_i(\mathbf{s})$, $\theta_{r_i}(\mathbf{s})$,

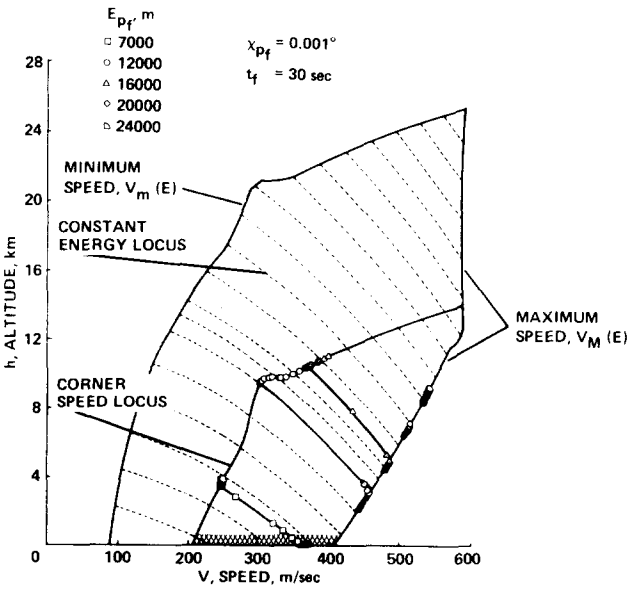

Fig. 4. Three-dimensional pursuer extremal trajectories in the flight envelope (F4-C, time marked at 1-s intervals).

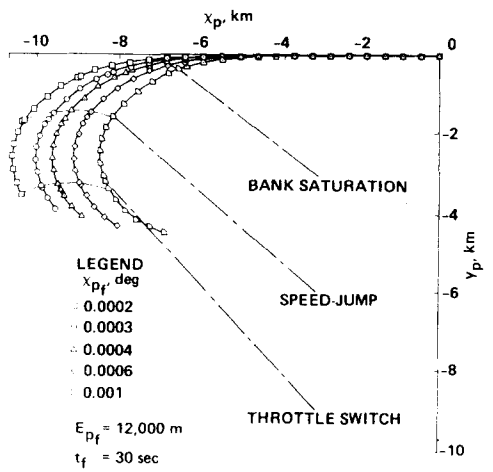

Fig. 5. Projection of three-dimensional energy-state trajectories on a horizontal plane (F4-C).

and $n_{r_i}(\mathbf{s})$, $i = \mathrm{p}, \mathrm{e}$. We may use this solution also to express the slow adjoint variables and the fast state and adjoint variables of each aircraft in terms of all the slow state variables. That is, we can form state-feedback laws $\Lambda_i(\mathbf{s})$, $h_{r_i}(\mathbf{s})$, $\gamma_{r_i}(\mathbf{s})$, $\lambda_{h_{r_i}}(\mathbf{s})$, and $\lambda_{\gamma_{r_i}}(\mathbf{s})$. It is these feedback expressions that are needed in the control algorithms derived in the following two sections.

4. NONLINEAR CONTROL LAW

When the state of a player is far away from the reduced solution, we use (6) as the basis for boundary-layer analysis of that player. Specifically, (6) is used when $|h - h_r(E)| > \delta$, where h is the current altitude, $h_r(E)$ is the reduced solution altitude at the current energy E, and δ is a preselected constant.

There are two boundary layers associated with (6), one for the altitude dynamics and one for the flightpath dynamics. These boundary layers are basically the same as those in [24], and we will follow that reference in our development. The difference is that in [24] the slow variables are further time-scale decoupled, whereas in our approach they are not. Because the termination condition is independent of the fast state variables h and γ, and because both the pursuer and the evader wish to minimize the transition times to, and between, branches of the reduced solution, the boundary-layer analysis that follows is independently valid for both players, and (for the most part) we do not use subscripts p and e.

The necessary conditions for minimum time control of system (6) may be written as

$$\begin{aligned} \dot{\mathbf{s}} &= H_{\lambda}, & \dot{\boldsymbol{\lambda}} &= -H_{\mathbf{s}} \\ \epsilon\dot{h} &= H_{\lambda_h}, & \epsilon\dot{\lambda}_h &= -H_h \\ \epsilon^2\dot{\gamma} &= H_{\lambda_\gamma}, & \epsilon^2\lambda_\gamma &= -H_\gamma \\ H_\beta &= 0, & H_\theta &= 0, \qquad H_n = 0, \qquad H = 0, \end{aligned} \tag{15}$$

where subscripts denote partial differentiation and where

$$H = A\cos\gamma + B - \lambda_E V D_i n^2 + \frac{\lambda_\chi g n \sin\theta}{V\cos\gamma} + \lambda_h V\sin\gamma + \frac{\lambda_\gamma g}{V}(n\cos\theta - \cos\gamma) + \mu_1(n - n_s) + \mu_2(n - \hat{L}) + \mu_3(\beta - 1) + \mu_4\beta \tag{16}$$

with

$$A(\mathbf{s}, \Lambda(\mathbf{s}), h) = \lambda_x V\cos\chi + \lambda_y V\sin\chi \qquad B(\mathbf{s}, \Lambda(\mathbf{s}), h, \beta(\mathbf{s})) = 1 + \lambda_E V(\beta T_M - D_0). \tag{17}$$

In (16), the μ_i are multipliers for the control constraints (3), $\hat{L}$ is given by (4), and D_i is defined by (2). Noting that the throttle control β is completely determined by the reduced solution, we have written $\beta(\mathbf{s})$ and we need not consider variations of β in the boundary layers.

The zero-order approximation to the altitude boundary layer is obtained by introducing the stretching transformation $\tau_1 = t/\epsilon$ into (15) and then setting $\epsilon = 0$:

$$\begin{aligned} \mathbf{s}' &= \mathbf{0}, & \boldsymbol{\lambda}' &= 0 \\ h' &= H_{\lambda_h}, & \lambda_h' &= -H_h \\ 0 &= H_{\lambda_\gamma}, & 0 &= -H_\gamma \\ H_\theta &= 0, & H_n &= 0, \qquad H = 0, \end{aligned} \tag{18}$$

where $(\quad)' = \mathrm{d}(\quad)/\mathrm{d}\tau_1$. The last five of these equations are, when written out in full,

$$n\cos\theta - \cos\gamma = 0$$

$$-A\sin\gamma + \frac{\lambda_\chi g n\sin\theta\sin\gamma}{V\cos^2\gamma} + \lambda_h V\cos\gamma + \lambda_\gamma\frac{g}{V}\sin\gamma = 0$$

$$\lambda_\chi\frac{\cos\theta}{\cos\gamma} - \lambda_\gamma\sin\theta = 0$$

$$-2\lambda_E VD_i n + \lambda_\gamma \frac{g \sin\theta}{V\cos\gamma} + \frac{\lambda_\chi g\cos\theta}{V} + \mu_1 + \mu_2 = 0$$

$$A\cos\gamma + B - \lambda_E VD_i n^2 + \frac{\lambda_\chi gn\sin\theta}{V\cos\gamma} + \lambda_h V\sin\gamma = 0. \tag{19}$$

These five algebraic equations may be used to eliminate γ, λ_γ, θ, and n and thereby to obtain an expression for the altitude adjoint in state-feedback form; we write this feedback law as

$$\Lambda_{h_i}(\mathbf{s}, h_i) = \lambda_{h_i}(\mathbf{s}_i, \Lambda_i(\mathbf{s}), h_i, \beta_i(\mathbf{s})) \quad i = \mathrm{p}, \mathrm{e}. \tag{20}$$

A general approach to the simultaneous solution of (19) may be found in [24]. Here, we will briefly illustrate (20) for the case of a bounded load factor "below" the corner speed, $V > V_c(E)$. In this case, $n = n_s$ and we further assume that $n_s \gg 1$ and $|\gamma| \ll 1$ (i.e. we set $\sin\gamma = \gamma$ and $\cos\gamma = 1$). Simultaneous solution of (19) then gives

$$\lambda_h = \pm\frac{1}{V}\left[\left(\frac{\lambda_\chi gn_s}{V} - A\right)\left(A + B + \frac{\lambda_\chi gn_s}{V} - \lambda_E VD_i n_s^2\right)\right]^{1/2} \tag{21}$$

which is in the form of (20).

Next we consider the γ boundary layer. The zero-order approximation is obtained by substituting $\tau_2 = t/\epsilon^2$ in (15) and then setting $\epsilon = 0$:

$$\begin{aligned} &\mathbf{s}'' = \mathbf{0}, && \boldsymbol{\lambda}'' = \mathbf{0} \\ &h'' = 0, && \lambda_h'' = 0 \\ &\gamma'' = H_{\lambda_\gamma}, && \lambda_\gamma'' = -H_\gamma \\ &H_\theta = 0, && H_n = 0, \quad H = 0, \end{aligned} \tag{22}$$

where $(\quad)'' = \mathrm{d}(\quad)/\mathrm{d}\tau_2$. The last three of these are the algebraic equations:

$$\lambda_\chi \frac{\cos\theta}{\cos\gamma} - \lambda_\gamma \sin\theta = 0$$

$$-2\lambda_E VD_i n + \frac{\lambda_\chi g\sin\theta}{V\cos\gamma} + \frac{\lambda_\gamma g\cos\theta}{V} + \mu_1 + \mu_2 = 0$$

$$A\cos\gamma + B - \lambda_E VD_i n^2 + \frac{\lambda_\chi gn\sin\theta}{V\cos\gamma} + \lambda_h V\sin\gamma + \frac{\lambda_\gamma g}{V}(n\cos\theta - \cos\gamma) = 0. \tag{23}$$

These equations are to be used to solve for θ and n as functions of all other variables except λ_γ. This results in algebraic state-feedback expressions for the controls, which we express as

$$\begin{aligned} \Theta_i(\mathbf{s}, h_i, \gamma_i) &= \theta_i(\mathbf{s}_i, h_i, \gamma_i, \Lambda_i(\mathbf{s}), \Lambda_{h_i}(\mathbf{s}, h_i), \beta_i(\mathbf{s})) \\ N_i(\mathbf{s}, h_i, \gamma_i) &= n_i(\mathbf{s}_i, h_i, \gamma_i, \Lambda_i(\mathbf{s}), \Lambda_{h_i}(\mathbf{s}, h_i), \beta_i(\mathbf{s})), \end{aligned} \tag{24}$$

where $i = \mathrm{p}$ for implementation by the pursuer and $i = \mathrm{e}$ for implementation by the evader.

To illustrate the solution of the γ boundary layer, we again consider the case $n = n_s \gg 1$, $|\gamma| \ll 1$; equations (23) then give the feedback controls as

$$\begin{aligned} \theta &= \sin^{-1}\left[\frac{\lambda_\chi gn_s}{V(\lambda_E VD_i n_s^2 - A - B - \lambda_h V\gamma)}\right] \\ n &= n_s, \end{aligned} \tag{25}$$

with λ_h given by (21). Equation (25) is in the form of (24).

A flow diagram of the implementation, for the pursuer, of the feedback control algorithm derived in this section is shown in Fig. 6. The most significant characteristic of the algorithm is that, as mentioned earlier, all the interaction between the two aircraft takes place in the reduced, or 3DES, solution. The opponent information enters the control laws via the functions $\Lambda(\mathbf{s})$ and $\beta(\mathbf{s})$. The purpose of the control laws Θ_p and N_p is, in effect, to drive the pursuing aircraft to its 3DES solution, under the assumption that the evading aircraft is always on its own 3DES solution. Finally, we note that the information needed for implementation by the pursuer consists of the values of all of the pursuer's state variables but of only the values of the evader's slow state variables.

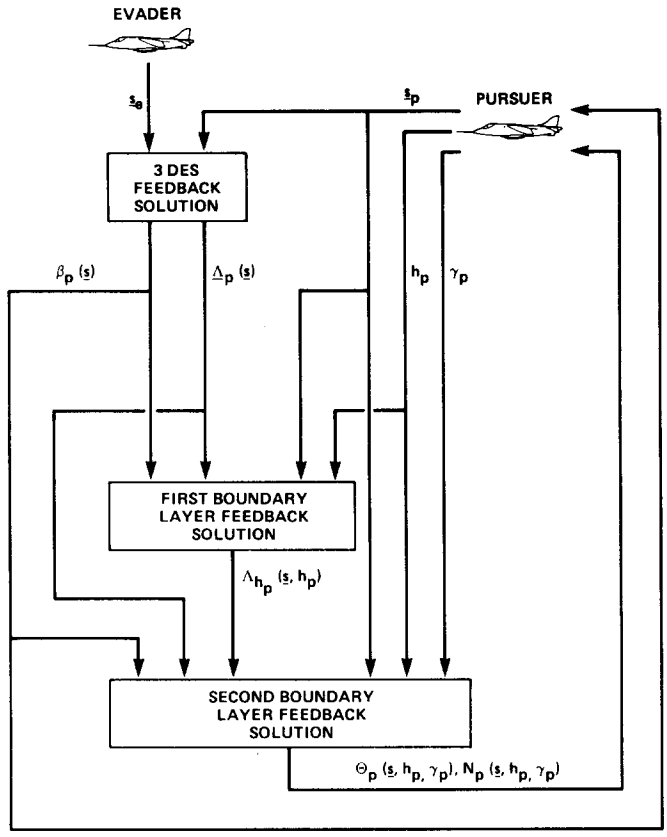

Fig. 6. Pursuer implementation of nonlinear state-feedback control, $|h_p - h_{r_p}(E_p)| > \delta$.

5. LINEAR CONTROL LAW

When the state of a player is near the reduced solution, $|h - h_r(E)| \leqslant \delta$, we adopt (9) for our boundary-layer model, to gain improved accuracy. Once again, because the boundary-layer motion is identical and independent for both players, we will not, for the most part, use subscripts p and e, with the understanding that the results will apply to either player.

The necessary condition for minimum-time control of system (9) are

$$\begin{aligned} \dot{\mathbf{s}} &= H_{\lambda}, \qquad \dot{\boldsymbol{\lambda}} = -H_{\mathbf{s}} \\ \epsilon \dot{f} &= H_{\lambda_f}, \qquad \epsilon \dot{\lambda}_f = -H_f \\ \epsilon \dot{\gamma} &= H_{\lambda_\gamma}, \qquad \epsilon \dot{\lambda}_\gamma = -H_\gamma \\ H_\beta &= 0, \qquad H_\theta = 0, \qquad H_n = 0, \qquad H = 0 \end{aligned} \tag{26}$$

where

$$H = A + B - \lambda_E V D_i n^2 + \frac{\lambda_\gamma g n \sin\theta}{V} + \lambda_f(\phi\gamma + \psi P) + \frac{\lambda_\gamma g\,(n\cos\theta - 1)}{V} + \mu_1(n - n_s) + \mu_2(n - \hat{L}) + \mu_3(\beta - 1) + \mu_4\beta \tag{27}$$

and where we have dropped the primes denoting functional dependence on E and f. As before, β is determined by the reduced solution, $\beta(\mathbf{s})$.

To obtain the zero-order approximation to the boundary-layer equations, we set $\tau_1 = t/\epsilon$ and then $\epsilon = 0$ in (26) to obtain

$$\begin{aligned} \mathbf{s}' &= 0, \quad \boldsymbol{\lambda}' = \mathbf{0} \\ f_b' &= \phi_b \gamma_b + \psi_b P_b \\ \lambda_{f_b}' &= -H_{f_b} \end{aligned}$$

$$\gamma_b' = g(n_b \cos\theta_b)/V_b$$
$$\lambda_{\gamma_b}' = -\lambda_{f_b}\phi_b$$
$$H_\theta = 0, \quad H_n = 0, \quad H = 0. \tag{28}$$

Because we are interested in obtaining control laws for use in the vicinity of the reduced solution, we will linearize (28) about the reduced solution, which is an equilibrium point of these equations [20].

Setting $\epsilon = 0$ in (26) gives the following algebraic expressions valid on the reduced solution:

$$0 = \phi_r \gamma_r + \psi_r P_r$$
$$0 = n_r \cos\theta_r - 1$$
$$0 = -H_{t_r}$$
$$0 = -\lambda_{f_r}$$
$$0 = \lambda_{\chi_r}\cos\theta_r - \lambda_{\gamma_r}\sin\theta_r$$
$$0 = -2\lambda_{E_r} V_r D_{i_r} n_r + \frac{\lambda_{\chi_r} g \sin\theta_r}{V_r} + \frac{\lambda_{\gamma_r} g \cos\theta_r}{V_r} + \mu_{1_r} + \mu_{2_r}$$
$$0 = A_r + B_r - \lambda_{E_r} V_r D_{i_r} n_r^2 + \frac{\lambda_{\chi_r} g n_r \sin\theta_r}{V_r}. \tag{29}$$

Expanding all fast state and adjoint variables and all control variables about their reduced values, then using (8) and (29) gives

$$f_b = f_r + \delta_f = \delta_f$$
$$\gamma_b = \gamma_r + \delta_\gamma = -\frac{\psi_r P_r}{\phi_r} + \delta_\gamma$$
$$\lambda_{f_b} = \lambda_{f_r} + \delta_{\lambda_f} = \delta_{\lambda_f}$$
$$\lambda_{\gamma_b} = \lambda_{\gamma_r} + \delta_{\lambda_\gamma}$$
$$n_b = n_r + \delta_n$$
$$\theta_b = \theta_r + \delta_\theta = \cos^{-1}\frac{1}{n_r} - \frac{(n_r^2 - 1)^{1/2}}{n_r^2 \lambda_{\gamma_r}}\delta_{\lambda_\gamma}. \tag{30}$$

Substituting (30) into (28), using (29), recalling that E and β are constant to zero-order in the boundary layer, and retaining only first-order terms in the perturbation variables δ_i gives

$$\delta_f' = a\delta_f + \phi\delta_\gamma - 2VD_i n\psi\delta_h$$
$$\delta_\gamma' = \frac{g(n^2-1)}{Vn^2\lambda_\gamma}\delta_{\lambda_\gamma} + \frac{g}{Vn}\delta_n$$
$$\delta_{\lambda_f}' = \left[-\frac{AV_{ff}}{V} - \lambda_E P_{ff} + \mu_2 \hat{L}_{ff} + \frac{g\lambda_\gamma(n^2-1)}{V^2}\left(V_{ff} - \frac{2V_f^2}{V}\right)\right]\delta_f - a\delta_{\lambda_f}$$
$$+ \left[2\lambda_E(V_f D_i + VD_{i_f}) + \frac{g\lambda_\gamma V_f}{V^2}\right] n\delta_n + \hat{L}_f \delta_{\mu_2}$$
$$\delta_{\lambda_\gamma}' = -\phi\delta_{\lambda_f} \tag{31}$$

where

$$a = \psi_f P + \psi P_f - \frac{\phi_f \psi P}{\phi}. \tag{32}$$

and where the subscript r has been dropped, with the understanding that all coefficients in (31) and (32) are to be evaluated on the reduced solution at the current, actual value of E.

Our procedure for deriving linear state-feedback control laws is now as follows. First, we solve

(31) for the perturbation variables, $\delta_i(\tau_1)$, and then evaluate the solutions at $\tau_1 = 0$, $\delta_i(0) = \delta_{i_0}$. In these calculations, we assume that the character of the load factor control does not vary locally; i.e. if it is bounded (unbounded) on the reduced solution it is bounded (unbounded) in the linearized boundary layer. The values δ_{i_0} are then used to construct feedback control laws via (30); these laws will be of the form

$$\begin{aligned}\Theta_i(\mathbf{s}, h_i, \gamma_i) &= \theta_{r_i}(\mathbf{s}) + \delta_{\theta_i}(\mathbf{s}_i, \Lambda_i(\mathbf{s}), h_i, \gamma_i, \beta_i(\mathbf{s}), h_{r_i}(\mathbf{s}), \gamma_{r_i}(\mathbf{s}), n_{r_i}(\mathbf{s}), \lambda_{\gamma_{r_i}}(\mathbf{s}))\\ N_i(\mathbf{s}, h_i, \gamma_i) &= n_{ri}(\mathbf{s}) + \delta_{n_i}(\mathbf{s}_i, \Lambda_i(\mathbf{s}), h_i, \gamma_i, \beta_i(\mathbf{s}), h_{r_i}(\mathbf{s}), \gamma_{r_i}(\mathbf{s}), n_{r_i}(\mathbf{s}), \lambda_{\gamma_{r_i}}(\mathbf{s}))\\ i &= \mathrm{p}, \mathrm{e}\end{aligned} \tag{33}$$

and will be linear in h_i and γ_i.

The solution of (31) will depend on the local nature of the reduced solution, as well as on whether the reduced load-factor control is bounded. There are not as many cases to consider as it would seem, however, since many combinations may be ruled out theoretically and others rarely occur in practice [21]. Here, we will illustrate the derivation of a control law for a specific case.

Suppose that the reduced solution is flight along a terrrain limit below the corner speed locus (the crosshatched locus in Fig. 4) and further suppose that the reduced load-factor control is bounded. For reduced flight along a terrain limit, h_T,

$$f = h - h_T, \quad f_h = 1, \quad f_V = 0, \quad \phi = V, \quad \psi = 0, \quad \gamma = 0, \quad a = 0, \quad V_f = -\frac{g}{V}, \quad V_{ff} = -\frac{g^2}{V^3}, \tag{34}$$

and for bounded load-factor control below the corner velocity

$$n = n_s, \quad \delta_n = 0, \quad \mu_2 = 0, \quad \delta_{\mu_2} = 0. \tag{35}$$

Consequently, (31) become, with $n_s \gg 1$,

$$\begin{aligned}\delta_f' &= V\delta_\gamma\\ \delta_\gamma' &= \frac{g}{V\lambda_\gamma}\delta_{\lambda_\gamma}\\ \delta_{\lambda_f}' &= C\delta_f\\ \delta_{\lambda_\gamma}' &= -V\delta_{\lambda_f},\end{aligned} \tag{36}$$

where

$$C = \frac{Ag^2}{V^4} - \lambda_E P_{hh} - \frac{3g^3\lambda_\gamma n_s^2}{V^5}. \tag{37}$$

If $CVg/\lambda_\gamma > 0$, then Theorem 2.2 of [20] is satisfied and the two stable modes have eigenvalues

$$s_{1,2} = -\frac{1}{(2)^{1/2}}\left(\frac{CVg}{\lambda_\gamma}\right)^{1/4} \pm \frac{i}{(2)^{1/2}}\left(\frac{CVg}{\lambda_\gamma}\right)^{1/4}. \tag{38}$$

To solve (36), we set

$$\delta_f = A_1\exp(st), \quad \delta_\gamma = A_2\exp(st), \quad \delta_{\lambda_f} = A_3\exp(st), \quad \delta_{\lambda_\gamma} = A_4\exp(st) \tag{39}$$

to get the mode shapes

$$\begin{aligned}A_3^{(i)} &= -\frac{s_i}{V}A_4^{(i)}\\ A_2^{(i)} &= \frac{g}{s_i V\lambda_\gamma}A_4^{(i)}\\ A_1^{(i)} &= \frac{g}{s_i^2\lambda_\gamma}A_4^{(i)},\end{aligned} \tag{40}$$

where s_i, $i = 1, 2$, are given by (38). Writing the solutions in terms of the two stable model shapes and evaluating at $\tau_1 = 0$ gives, in view of (30) and (40),

$$f_c = \frac{g}{\lambda_\gamma}\left(\frac{A_4^{(1)}}{s_1^2} + \frac{A_4^{(2)}}{s_2^2}\right)$$

$$\gamma_c = \frac{g}{V\lambda_\gamma}\left(\frac{A_4^{(1)}}{s_1} + \frac{A_4^{(2)}}{s_2}\right)$$

$$\delta_{\lambda_{f_0}} = -\frac{1}{V}(s_1 A_4^{(1)} + s_2 A_4^{(2)})$$

$$\delta_{\lambda_{\gamma_0}} = A_4^{(1)} + A_4^{(2)}, \tag{41}$$

where subscript c denotes current values. Solving the first two of these for $A_4^{(1)}$ and $A_4^{(2)}$ and substituting into the last gives

$$\delta_{\lambda_{\gamma_0}} = \frac{\lambda_\gamma}{g}[-s_1 s_2 f_c + V(s_1 + s_2)\gamma_c]. \tag{42}$$

Putting this expression in the last of (30) and using (38),

$$\delta_{\theta_0} = -\frac{1}{n_s \lambda_\gamma}\delta_{\lambda_{\gamma_0}}$$

$$\delta_{\theta_0} = \left(\frac{4V_r C_r}{g^3 n_s^4 \lambda_{\gamma_r}}\right)^{1/4}\left[\left(\frac{gV_r C_r}{4\lambda_{\gamma_r}}\right)^{1/4}(h_c - h_T) + V_r\gamma_c\right], \tag{43}$$

where subscript r has been added to emphasize that the coefficients in this equation are to be evaluated on the reduced solution at the current value of energy, E_c. Finally, the controls to be implemented are

$$\theta = \cos^{-1}\frac{1}{n_s} + \delta_{\theta_0}$$

$$n = n_s \tag{44}$$

From (43) we see that δ_{θ_0} is proportional to deviations from reduced solution values for both f and γ and that use of the control law (44) will tend to drive the state toward the reduced solution.

A flow diagram of the implementation for the pursuer of the control algorithm method discussed in this section is shown in Fig. 7.

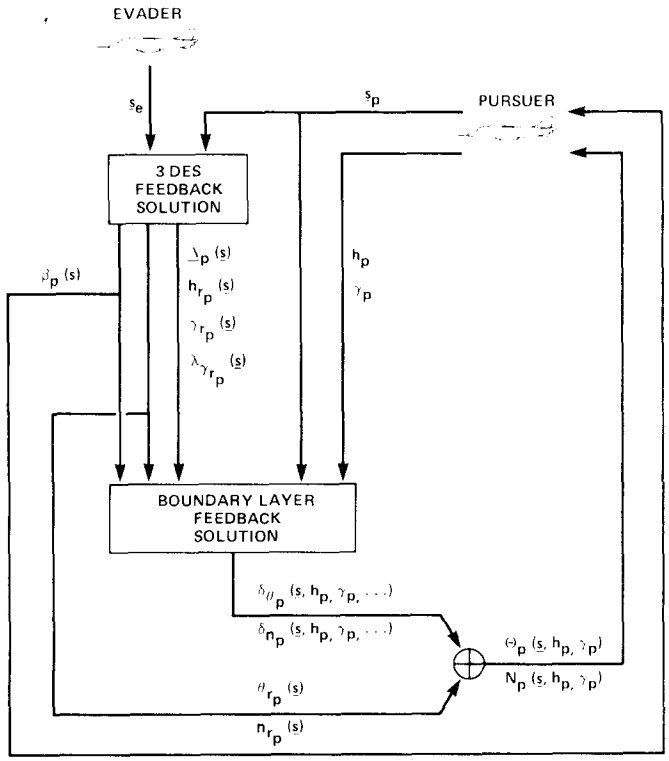

Fig. 7. Pursuer implementation of linear state feedback control, $|h_p - h_{r_p}(E_p)| \leq \delta$.

6. IMPLEMENTATION ISSUES

Past pursuit–evasion differential game solutions have not been useful in practical aircraft control applications, primarily because the dynamic models used were too simple. In the most ambitious analysis, the three-dimensional energy-state (3DES) dynamic model was used, and in the present paper we have derived feedback control algorithms that are based on the 3DES pursuit–evasion solution. Specifically, time-scale separations have been introduced such that the 3DES appears as the reduced system of the singularly perturbed point-mass equations. Our guiding principle is to use as few time-scales as possible and still leave the problem tractable. For current states "far away" from the 3DES solution, time-scale decoupling of the two fast variables is required to arrive at a nonlinear algebraic state-feedback law for the controls. When the state is "close" to the 3DES solution, we make a change of fast variable, keep both fast variables on the same time-scale, and derive a linear feedback law for control increments to be added to the 3DES controls.

Most of the technical and computational complexity of the algorithm resides in the 3DES problem; the algebraic feedback laws resulting from the boundary-layer analysis are quite simple. A key assumption is that the capture condition is defined in terms of only the slow variables. Consequently, it is in the 3DES solution that assumptions regarding the player's roles (pursuer, evader, interceptor) enter into the algorithm, that capturability is determined, and that barrier surfaces and other typical differential game phenomena arise. The computational task of constructing 3DES feedback solutions is formidable; however, this computation may be done off-line and the results converted to tabular data for on-board use.

There are two issues connected with our general approach that need further consideration. The first is the treatment of the instantaneous jumps between the branches of the 3DES solution, a consequence of modeling the altitude h as a fast variable. In our approach, we have implicitly assumed that when one of these jumps is reached, a switch to the nonlinear control law, with the new reduced values as equilibrium point, is made. It is clear that in terms of more closely following the 3DES solution, it would be better to anticipate the jump by switching control laws earlier, but there are no guidelines for this. In the context of the singularly perturbed point-mass equations, these jumps are interior transition layers, and what is needed is a detailed investigation of these layers for the three-dimensional case. Transition layers for two-dimensional (vertical plane) flight have been studied computationally on one time-scale [35] and analytically on two time-scales [36, 37].

The other issue is a consequence both of modeling h as a fast variable and of our key restriction that capture is specified only in terms of slow variables. Placing constraints on the final energies of the two players limits their possible final altitudes, but the range of possible values may still be great. Consequently, the difference between the altitudes of the aircraft at termination may be substantial, the implicit assumption being that the pursuer's weapon is able to close this altitude gap. If this assumption is not valid, the pursuer must reduce the altitude difference to a prespecified value, while the evader attempts to prevent this.

There are several possible approaches to including an altitude-matching requirement, the most obvious of which is to relax our key restriction and impose a maximum altitude difference as part of the capture criteria. The altitude-matching requirement would then lead to a terminal boundary layer, of necessity coupled between the two players; this would change the entire structure of the problem and make it much more complex. Second, we may define an independent "end-game", to be initiated when "capture", in the 3DES sense, has been achieved. If energy-state modeling is used for this end-game, conceptual complexities arise, such as the need to consider the relative informational advantages of the players [7]. It may even happen that the pursuer is not able to close the altitude gap to the required value, implying successful evasion and thereby contradicting the capturability conclusion of the 3DES game. Finally, we may use a heuristic engineering approximation to model terminal altitude changes [25]. If altitude match proves to be an issue, further investigation will be required to determine the best resolution.

7. CONCLUDING REMARKS

In summary, we have outlined an approach to three-dimensional aircraft pursuit–evasion that has potential use for an on-board automatic controller. The dynamic model and time-scale

assumptions should give realistic results, and the computational requirement should be well within real-time calculation. To validate the algorithm, it would be highly desirable to compare its performance with that of open-loop optimal solutions of the full point-mass model, to conduct comprehensive simulations, and, eventually, to flight test it.

REFERENCES

1. R. Isaacs, *Differential Games*. Wiley, New York (1965).
2. A. W. Merz, The game of two identical cars. *Multi-criteria Decision-Making and Differential Games*. Plenum Press, New York (1976).
3. J. V. Breakwell and A. W. Merz, Minimum required capture radius in a coplanar model of the aerial combat problem. *AIAA J.* **15**, Aug. (1977).
4. A W. Merz and D. S. Hague, Coplanar tail-chase aerial combat as a differential game. *AIAA J.* **15**, Oct. (1977).
5. A. W. Merz, To pursue or to evade—that is the question. *J. Guid. Control Dynam.* **8**, Mar. Apr. (1985).
6. H. J. Kelley, Differential-turning optimality criteria. *J. Aircraft* **12**, Jan. (1975).
7. H. J. Kelley, Differential-turning tactics. *J. Aircraft* **12**, Dec. (1975).
8. H. J. Kelley and L. Lefton, Computation of differential-turning barrier surfaces. *J. Spacecraft Rockets* **14**, Feb. (1977).
9. H. J. Kelley, Differential-turn maneuvering. *Automatica* **12**, May (1976).
10. M. D. Ardema, Air-to-air combat analysis: review of differential game approaches. Presented at the *1981 Joint Automatic Control Conference*, Charlottesville, Va (1981).
11. N. Rajan, U. R. Prasad and N. J. Rao, Pursuit-evasion of two aircraft in a horizontal plane. *J. Guid. Control* **3**, May June (1980).
12. U. R. Prasad, N. Rajan and N. J. Rao, Planar pursuit evasion with variable speeds, Pt. 1, extremal trajectory maps. *J. Optim. Theory Applic.* **33**, Mar. (1981).
13. N. Rajan, U. R. Prasad and N. J. Rao, Planar pursuit evasion with variable speeds, Pt. 2, barrier sections. *J. Optim. Theory Applic.* **33**, Mar. (1981).
14. N. Rajan and M. D. Ardema, Computation of optimal feedback strategies for interception in a horizontal plane. *J. Guid. Control Dynam.* **7**, Sept. Oct. (1984).
15. N. Rajan and M. D. Ardema, Barriers and dispersal surfaces in minimum-time interception. *J. Optim. Theory. Applic.* **42**, Feb. (1984).
16. K. H. Well, B. Faber and E. Berger, Optimization of tactical aircraft maneuvers utilizing high angles of attack. *J. Guid. Control* **5**, Mar. Apr. (1982).
17. B. S. A. Jarmark, A. W. Merz and J. V. Breakwell, The variable-speed tail-chase aerial combat problem. *J. Guid. Control* **4**, May–June (1981).
18. H. J. Kelley, Aircraft maneuver optimization by reduced order approximations. *Advances in Control and Dynamic Systems*, Vol. 10. Academic Press, New York (1973).
19. M. D. Ardema, Solution of the minimum time-to-climb problem by matched asymptotic expansions. *AIAA J.* **14**, July (1976).
20. M. D. Ardema (Ed.), An introduction to singular perturbations in nonlinear optimal control. *Singular Perturbations in Systems and Control*. Courses and Lectures No. 280, International Centre for Mechanical Sciences, Udine, Italy (1983).
21. N. Rajan and M. D. Ardema, Interception in three dimensions: an energy formulation. *J. Guid. Control Dynam.* **8**, Jan. Feb. (1985).
22. A. J. Calise, Singular perturbation methods for variational problems in aircraft flight. *IEEE Trans. Automat. Control.* **AC-21**, June (1976).
23. A. J. Calise, Extended energy management methods for flight performance optimization. *AIAA J.* **15** (1977).
24. A. J. Calise and D. D. Moerder, Singular perturbation techniques for real time aircraft trajectory optimization and control. NASA CR-3497 (1982).
25. J. Shinar, N. Farber and M. Negrin, A three-dimensional air combat game analysis by forced singular perturbations. AIAA Paper 82-1327 (1982).
26. H. J. Kelley, E. M. Cliff and A. R. Weston, Energy state revisited. AIAA Paper 83-2138 (1983).
27. M. D. Ardema and N. Rajan, Slow and fast state variables for three-dimensional flight dynamics. *J. Guid. Control Dynam.* **8**, July Aug. (1985).
28. M. D. Ardema and N. Rajan, Separation of time scales in aircraft trajectory optimization. *J. Guid. Control Dynam.* **8**, Mar. Apr. (1985).
29. D. B. Price, A. J. Calise and D. D. Moerder, Piloted simulation of an algorithm for on-board control of time-optimal intercept. NASA TP-2445 (1985).
30. M. D. Ardema, M. Heymann and N. Rajan, Combat games. *J. Optim. Theory Applic.* **46**, Aug. (1985).
31. M. Heymann, M. D. Ardema and N. Rajan, A formulation and analysis of combat games. NASA TP-2487, June (1985).
32. M. D. Ardema, M. Heymann and N. Rajan, Analysis of a combat problem: the turret game. Submitted to *J. Optim. Theory Applic.*
33. M. Heymann, N. Rajan and M. D. Ardema, On optimal strategies in event-constrained differential games. Presented at the *24th IEEE Conference on Decision and Control*, Fort Lauderdale, Fla. (1985).
34. M. D. Ardema, Singular perturbations in flight mechanics. NASA TM X-62,389, 2nd ed. (1977).
35. A. R. Weston, E. M. Cliff and H. Kelley, Altitude transitions in energy climbs. *Automatica* **19**, Feb. (1983).
36. J. V. Breakwell, Optimal flight-path-angle transitions in minimum-time airplane climbs., *J. Aircraft* **14**, Aug. (1977).
37. J. V. Breakwell, More about flight-path-angle transitions in optimal airplane climbs. *J. Guid. Control* **1**, May–June (1978).